Electronic Supplementary Material (ESI) for Nanoscale.

Supplementary Information

Hierarchical Network Relaxation of Dynamic Cross-Linked Polyolefin Elastomer for Advanced Reversible Shape Memory Effect

Zhao Xu,[†] Sen Meng,[†] Dun-Wen Wei,[‡] Rui-Ying Bao,[*,†] Yu Wang,[†] Kai Ke,[†] Wei Yang[*,†]

[†]College of Polymer Science and Engineering, Sichuan University, State Key Laboratory of Polymer Materials Engineering, Chengdu, 610065, Sichuan, China

[‡]School of Mechanical and Electrical Engineering, University of Electronic Science and Technology of China, Chengdu, 611731, Sichuan, China

[*]Corresponding authors. Tel/Fax: + 86 28 8546 0130.

E-mail addresses: rybao@scu.edu.cn (RY Bao) and weiyang@scu.edu.cn (W Yang)

Characterization

Fourier transform-infrared spectroscopy.

The chemical structure of POEV was characterized by Fourier transform-infrared spectrometer (FTIR, 6700, Nicolet Instrument Company, USA) in the wavenumber range from 4000 to 400 cm^{-1} with a resolution of 4 cm^{-1} in transmission mode.

Rheological tests.

Rheological measurements were carried out on a stress-controlled rotational rheometer (AR2000EX, TA instruments, USA) in a dynamic frequency sweep from 0.01 to 100 Hz at a strain of 1% within the linear viscoelastic region at 120 °C.

Gel content

The gel content was measured by soxhlet extraction. 0.3 g sample wrapped in a polytetrafluoroethylene (PTFE) filter membrane was immersed in n-heptane. Soxhlet extraction was carried out at 130°C for 10 h. The extracted samples were dried in a vacuum oven to remove the solvent. The gel content was calculated by the ratio of the mass of insoluble content to initial mass of the sample according to equation:

$$Gel\ content = \frac{w_i}{w_0} \times 100\%$$

where w_0 and w_i are the quality of the sample before and after extraction, respectively.

One-dimensional wide-angle X ray diffraction.

One-dimensional wide-angle X-ray diffraction (1D-WAXD) were carried out with a DX-1000 diffractometer with Cu Kα radiation (λ = 0.154 nm) at a voltage of 40 kV and a current of 40 mA. Samples were scanned over the range of diffraction angle 2θ = 5-80º, with a speed of $10^{o} \cdot min^{-1}$ at room temperature.

Orientation parameter.

The orientation parameter of POE crystallites was estimated using Herman's alignment, which is defined as follows[1]:

$$f = (3(\cos^2\varphi) - 1)/2$$

where $(\cos^2 \varphi)$ is the alignment factor defined as

$$(cos^2\varphi) = \int_0^{\pi/2} I(\varphi) \cos^2\varphi \sin\varphi \, d\varphi / \int_0^{\pi/2} I(\varphi) \sin \varphi \, d\varphi$$

where φ is the azimuth angle, and $I(\varphi)$ is the diffraction intensity corresponding to the azimuth angle φ.

Two-dimensional small-angle X-ray scattering (2D-SAXS).

Two-dimensional small-angle X-ray scattering (2D-SAXS) were performed at the SAXS instrument Xeuss 2.0 (France).

Scanning electron microscopy.

The morphologies of samples were characterized by scanning electron microscope (SEM, JEOL JSM-5900LV). The sample was cryo-fractured in liquid nitrogen. Then the cross-section was sputter-coated with gold prior to examination.

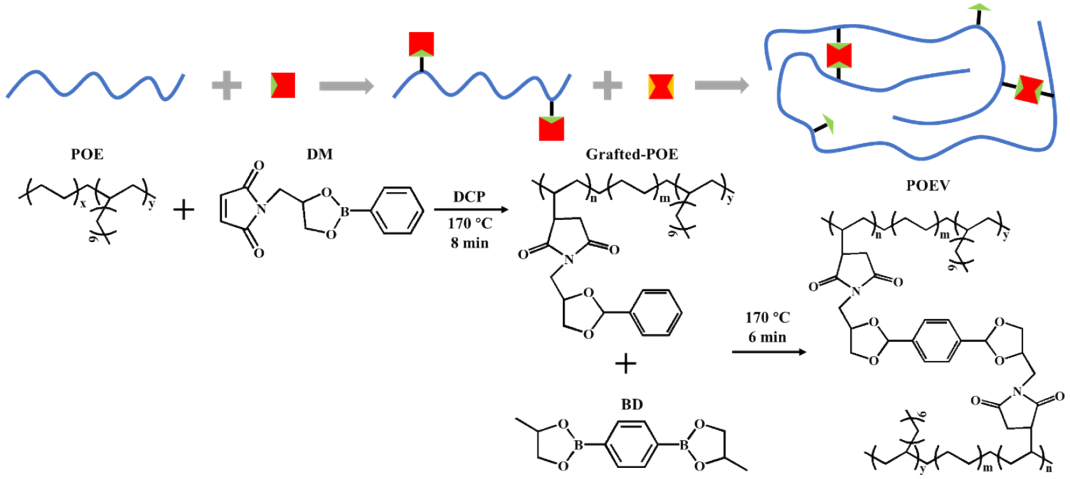

Figure S1 Schematic illustration for the preparation of POEV.

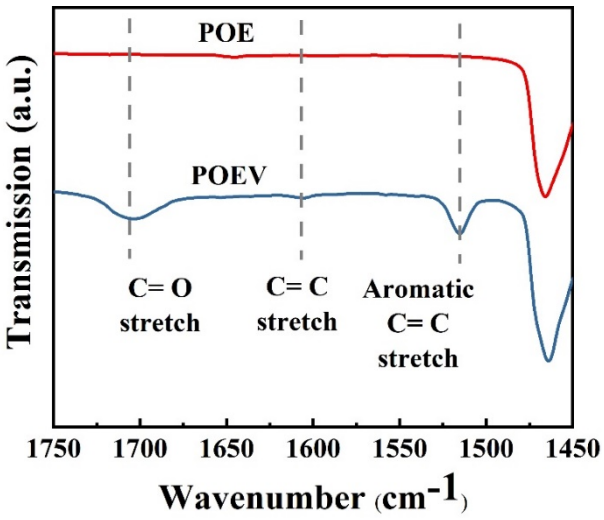

Figure S2 FTIR spectra of neat POE and POEV.

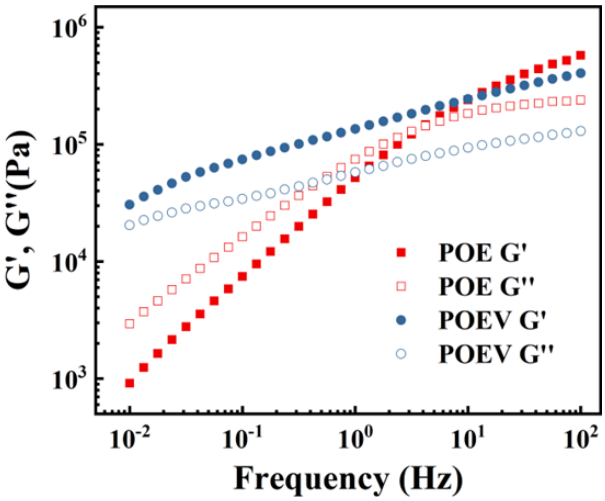

Figure S3 Variation of storage modulus (G′) and loss modulus (G″) as functions of frequency for POE and POEV by rheological measurements.

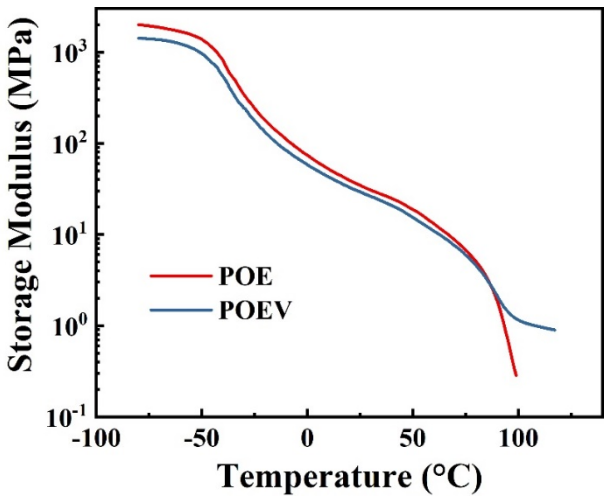

Figure S4 Storage modulus as a function of temperature for POE and POEV.

Table S1. The gel content of POE and POEV.

Samples	Gel content (%)
POE	0
POEV	84.6

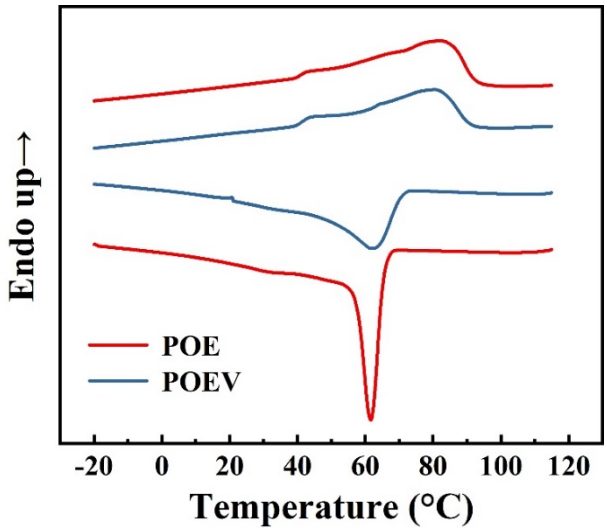

Figure S5 DSC cooling and second heating curves of POE and POEV.

Table. S2 Parameters from DSC melting and cooling scans of POE and POEV.

Samples	T_c (°C)	T_m (°C)	ΔH_m (J·g^{-1})	X_c %
POE	61.6	82.3	37.7	12.9
POEV	62.1	80.6	34.0	11.6

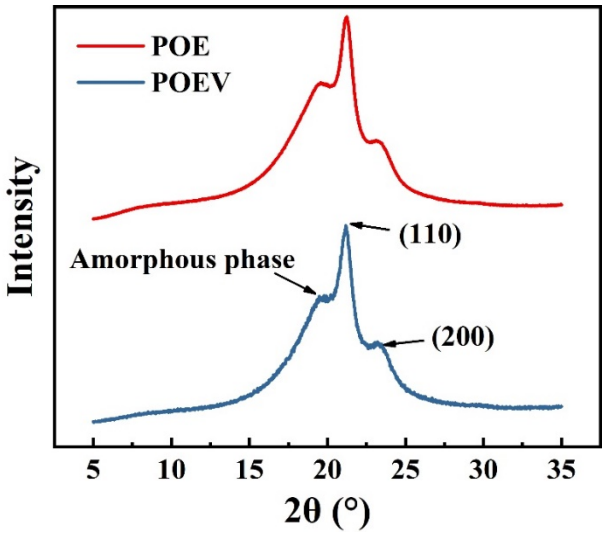

Figure S6 1D-WAXD curves of POE and POEV.

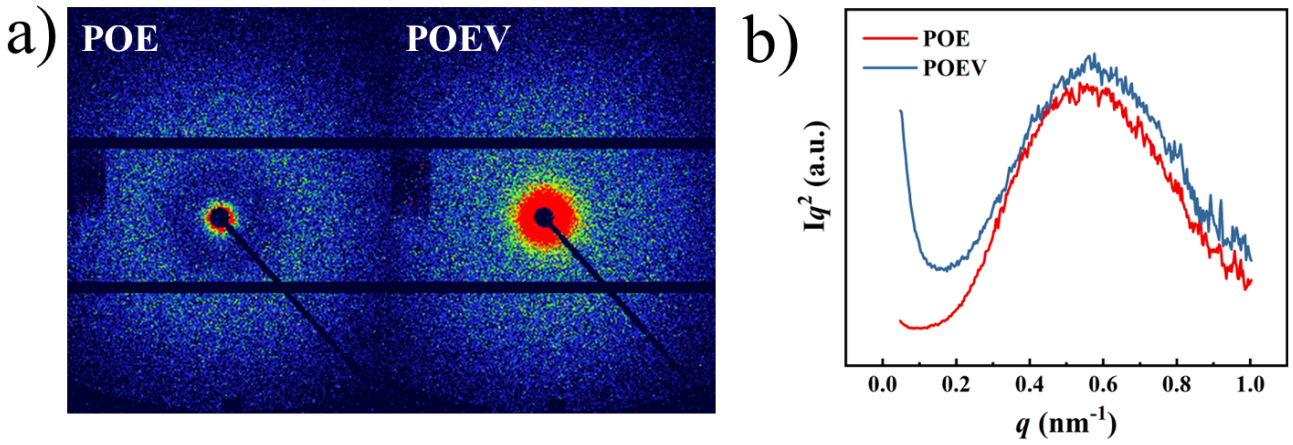

Figure S7 (a) 2D-SAXS patterns and (b) Iq^2 vs. q curves of POE and POEV.

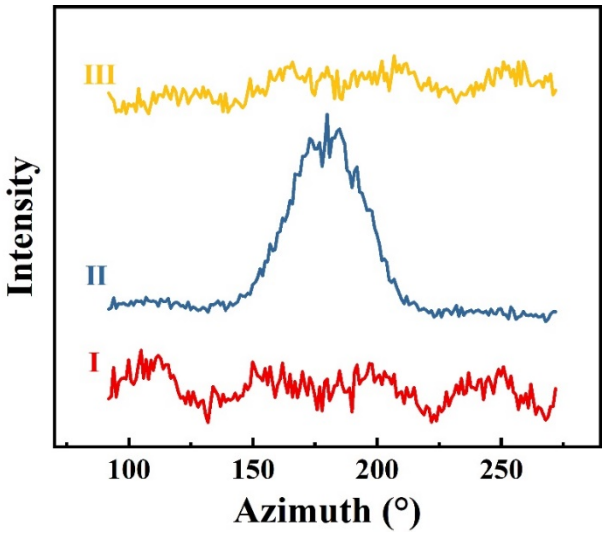

Figure S8 The scattering intensity vs. azimuthal profiles of (110) plane from the patterns in Figure 1c.

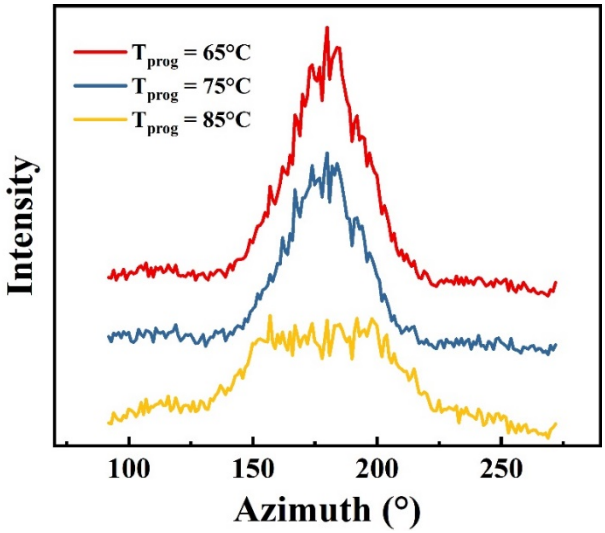

Figure S9 The scattering intensity vs. azimuthal profiles of (110) plane from the patterns in Figure 2b.

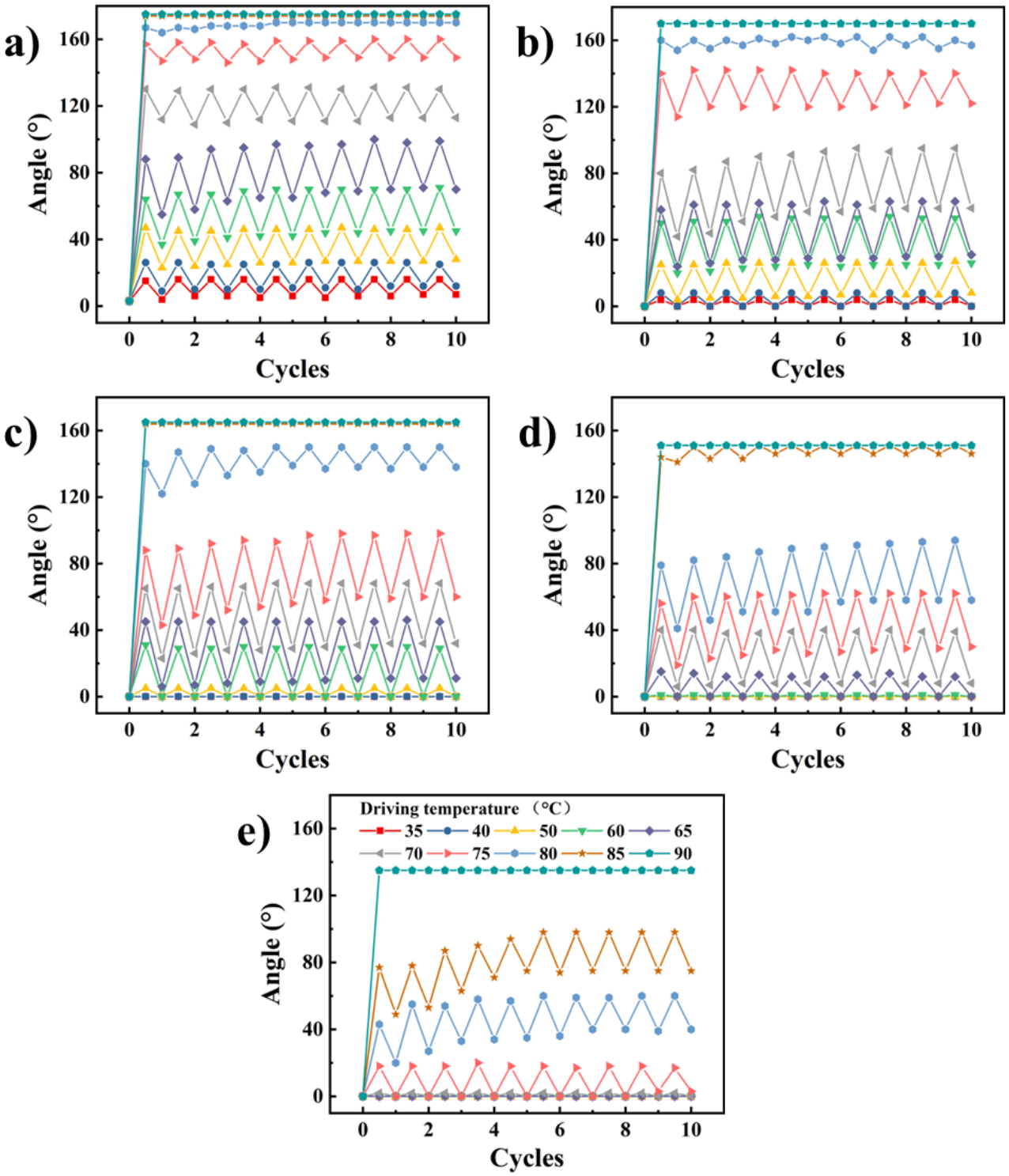

Figure S10 The angle change between 5 °C and varied driving temperatures for POEV programmed at (a) 65 °C, (b) 70 °C, (c) 75 °C, (d) 80 °C and (e) 85 °C, respectively.

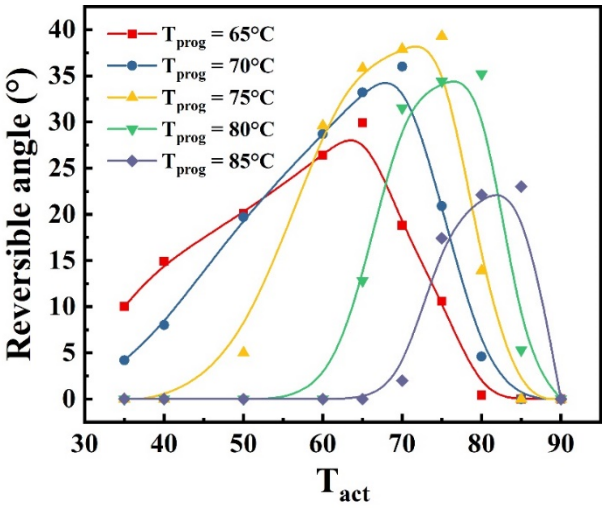

Figure S11 The average reversible angle change of clips made from POEV with different T_{prog} as a function of T_{act}.

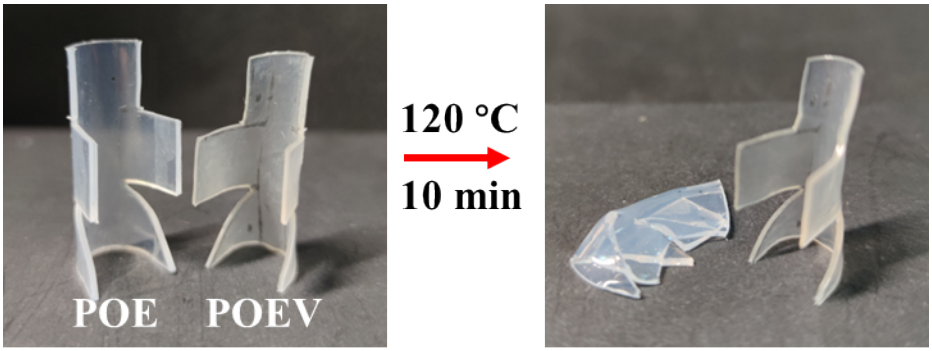

Figure S12 Shape stability of POE and POEV at high temperature.

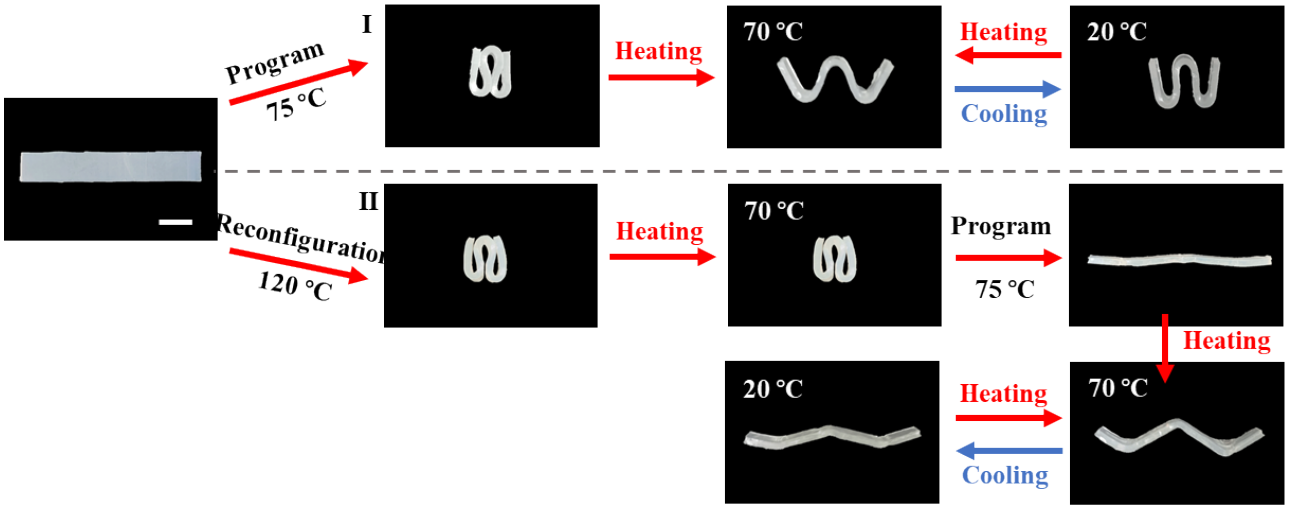

Figure S13 "W" shape-shifting realized by reversible shape memory effect (I), and converse reversible shape memory effect through varied programming procedures benefiting from the reconfigurability of POEV (II).

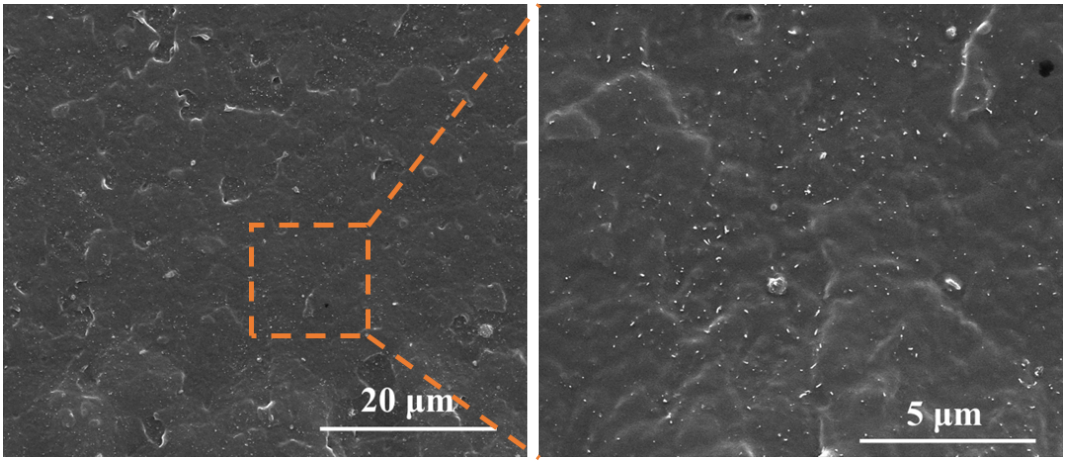

Figure S14 SEM images of POEV/CNT composites.

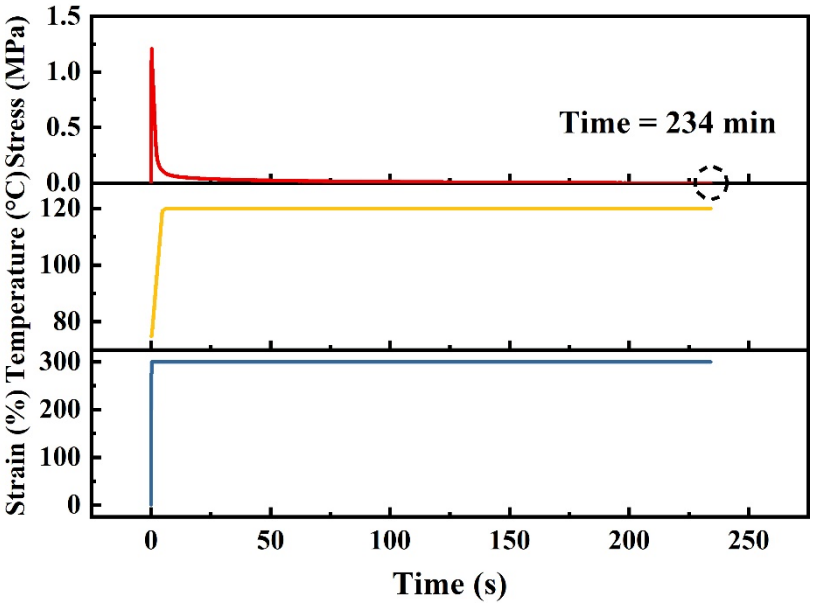

Figure S15 Stress relaxation of POEV/CNT composites with 300% strain at 120 °C.

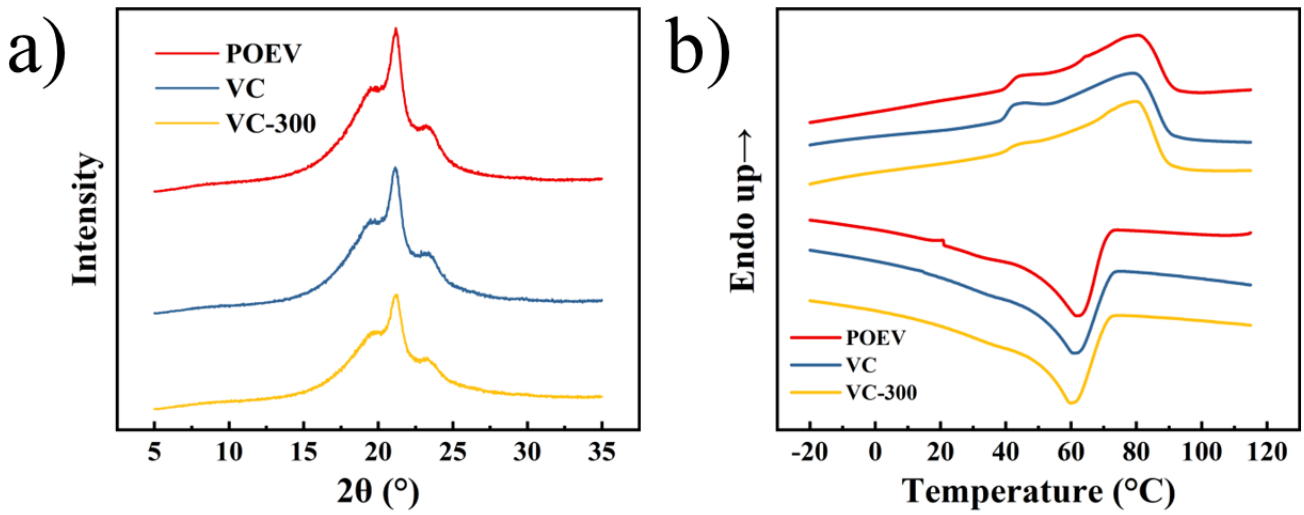

Figure S16 (a) 2D-WAXD and (b) DSC curves of POEV and POEV/CNT composites.

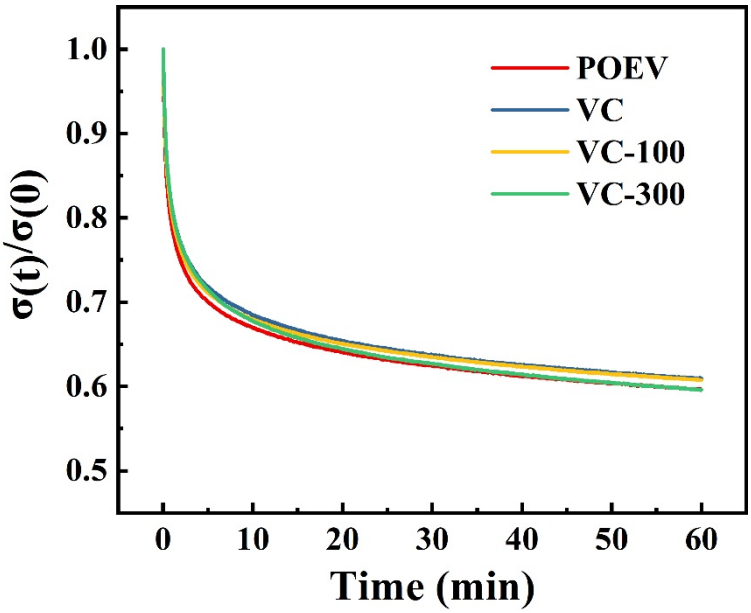

Figure S17 Stress relaxation behaviors of POEV and POEV/CNT composites.

References

1. S. J. Picken, J. Aerts, R. Visser and M. G. Northolt, *Macromolecules*, 1990, **23**, 3849-3854.